Colloid Polym Sci 277:34–40 (1999)

ORIGINAL CONTRIBUTION

K. Aramaki
H. Kunieda

Solubilization of oil in a mixed cationic liquid crystal

Received: 20 April 1998
Accepted: 16 July 1998

K. Aramaki · H. Kunieda (✉)
Graduate School of Engineering,
Yokohama National University,
Tokiwadai 79-5, Hodogaya-ku,
Yokohama 240-8501, Japan

Abstract The mixing fraction of didodecyldimethylammonium bromide (DDAB) in dodecyltrimethylammonium bromide + DDAB to produce a lamellar liquid crystal (L_α) abruptly decreases upon addition of a small amount of *m*-xylene, whereas the mixing fraction becomes constant at high *m*-xylene content. Similar results were obtained in saturated hydrocarbon systems. It is considered that oil molecules in the surfactant palisade layer increases the effective cross-sectional area per surfactant head group, a_s, whereas a_s is constant if the oil molecules are solubilized in the core of the liquid crystal. The volume fraction of penetrating oil in the total solubilized oil is defined as a penetration parameter, Pe, which is calculated from small-angle X-ray scattering data. Pe is high in the *m*-xylene system, whereas it is low in the *n*-decane system. Even in the same oil system, Pe decreases dramatically with increasing solubilization. Hence, most of the oil added penetrates into a palisade layer at an early stage of oil addition. This causes a change in the mixing fraction of surfactant in the L_α phase. Thereafter the oil is solubilized in the core of the bilayer with further addition of oil.

Key words Oil penetration – Phase behavior – Small-angle X-ray scattering – Lamellar liquid crystal – Cationic surfactant

Introduction

It is known that the hydrophile-lipophile balance (HLB) temperature of a polyoxyethylene-type nonionic surfactant system increases with long-chain saturated hydrocarbons and shifts to lower temperatures with cyclic or aromatic hydrocarbons [1, 2]. This phenomenon can be understood by the difference in the degree of oil penetration into a surfactant layer since penetration forces the spontaneous negative curvature of a surfactant layer and this is enhanced by oils with smaller molecular size or by polar oils [3]. It is reported that the amount of oil added to induce a rod-globule transition of micellar structure increases with long-chain hydrocarbons [4]. This can also be understood by the weak penetration of a long-chain oil.

Oil penetration has been observed directly by SANS experiments in several microemulsion systems with deuterated solvents [5–7]. Scattering-length density varies gradually across a monolayer, which is evidence of solvent penetration into the surfactant monolayer.

To tune the HLB of a surfactant, a medium-chain alcohol is often admixed as a cosurfactant with a hydrophilic surfactant [4]. The hydrocarbon chain length of the cosurfactant used is usually shorter than that of the surfactant. Oil penetration into a surfactant layer increases, if the two hydrocarbon chains of a double-tail surfactant are asymmetric [7]. Therefore, when the combination of long-tail surfactant and medium-chain alcohol is used, the degree of penetration is affected not only by the HLB of the mixed surfactant but also by the difference in the lipophilic

chain lengths. Moreover, alcohol molecules are located not only in the mixed surfactant layer but also in a separated bulk-oil phase or a micro-oil domain inside surfactant aggregates in both nonionic and ionic surfactant systems [8, 9]. The solubility of alcohol in oil is rather high, i.e., more than several weight percent to oil. In the case of mixed nonionic surfactants, the distribution of component surfactants also takes place [10, 11]. Hence, it is difficult to figure out the oil penetration in these ionic surfactant-cosurfactant and mixed nonionic surfactant systems. On the contrary, a mixture of didodecyltrimethylammonium bromide (DTAB) and didodecyldimethylammonium bromide (DDAB) is suitable for studying oil penetration because both surfactants have almost the same head group and tail length and are scarcely soluble as monomers in both water and oil.

The phase behavior and the microstructures of microemulsions of double-tail cationic surfactants such as DDAB have been extensively studied [12–16]. Lamellar liquid crystals (L_α) are formed over almost the whole composition range in the binary water/DDAB system. Upon addition of hydrocarbons to L_α water-in-oil (w/o)-type microemulsions are formed due to oil penetration. The degree of oil penetration was estimated by the volume ratio of surfactant plus penetrating oil to surfactant in the DDAB systems [13]. However, it was assumed that surfactant length in a L_α is equal to that in a reverse-curved microemulsion and that the effective cross-sectional area per surfactant is not changed by oil penetration. Since it is reported that the surfactant length changes dramatically when the structural transition of surfactant aggregates occurs [17] and the area per surfactant is increased by oil penetration [5], the above assumption does not hold in a real system.

In this paper, we report the degree of oil penetration in a bilayer of a L_α in the mixed DTAB-DDAB system by means of a phase study and small-angle X-ray scattering (SAXS) measurements.

Experimental section

Materials

Certified grade DTAB and DDAB were obtained from Tokyo Kasei Kogyo Co. and Kodak Co., respectively. Short and long single-tail and double-tail homologues (Tokyo Kasei Kogyo Co.) of the above cationic surfactants were used only for density measurements. These ionic surfactants were stored under vacuum with P_2O_5. Certified grade *m*-xylene, *n*-octane, *n*-decane, *n*-dodecane, and *n*-tetradecane were also obtained from Tokyo Kasei Kogyo Co. Distilled water was used. These chemicals were used without further purification.

Density measurement

Surfactant densities were measured at 25°C by a disital density meter, Anton Paar model DMA40. Since both surfactants were in a solid state, the densities of their methanol or ethanol solutions were measured at various surfactant concentrations. The reciprocals of these values were plotted against alcohol concentration and the densities of the pure surfactants in the liquid state were estimated from the intercepts of the density lines at 100% surfactant concentration.

Determination of the volume of the lipophilic part of DTAB and DDAB

We estimated the molar volumes of various monoalkyltrimethyl- and dialkyldimethylammonium bromides. The number of methylene units plotted against the molar volumes is shown in Fig. 1. Note that the unit for double-tail surfactants is two methylene groups.

Since a straight line can be fitted well for each series, the volume of a methylene unit is determined from the slopes of the fitted lines, 16.4 cm^3/mol for single-tail surfactants and 33.8 cm^3/mol (the volume of two methylene groups) for double-tail surfactants. The molar volumes of methyl and methylene units of alkanes, 33.0 and 16.5 cm^3/mol, respectively are calculated from the density measurement with successive change of alkane chain length. We can obtain the molar volume of the lipophilic part, 213.4 nm^3/mol for DTAB and 437.8 nm^3/mol for DDAB, by linear combination of the methylene volume in Fig. 1 and the molar volume of the methyl group(s) of the alkanes described above. The volume of the lipophilic part of DTAB is almost the

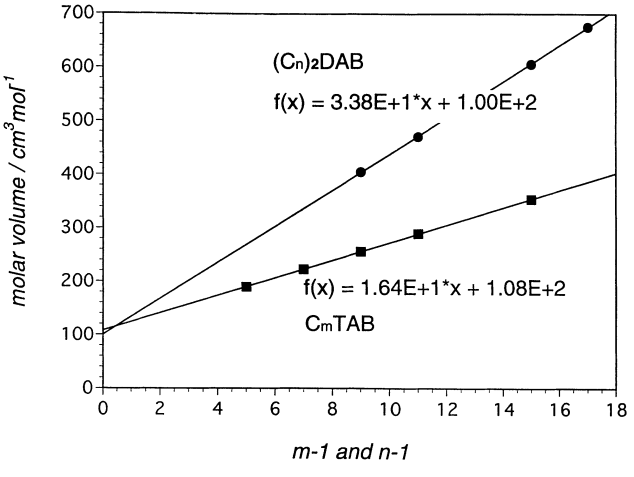

Fig. 1 Molar volume of alkyl quaternary ammonium bromide, single-tail homologues, C_mTAB (*filled squares*) and double-tail homologues, $(C_n)_2DAB$ (*filled circle*)

same as the sum of the methyl and methylene volumes of alkanes, but such additivity does not hold completely for DDAB, i.e., the lipophilic volume obtained is larger than expected. It may be due to steric hindrance of the tails of DDAB.

Phase diagrams

Various amounts of reagents were sealed in glass ampoules and they were kept in a thermostat after mixing. The phase state was determined by visual observation. L_α were detected by crossed polarizers and the peak ratio of SAXS [19].

SAXS measurements

The interlayer spacing of a L_α was determined from the first-order peak of the SAXS spectrum using Bragg's equation. Samples were sandwiched between two layers of polyethylene terephthalate film, and a Rigaku RINT 2500 spectrometer was used. The power generated for the measurements was 15 kW.

Results and discussion

Phase behavior of the water/DTAB/DDAB/*m*-xylene system

To understand how the addition of oil affects the phase behavior of the DTAB-DDAB system, we constructed the phase diagram at the constant volume fraction of the lipophilic part of the mixed surfactant in aqueous surfactant solution (Fig.2).

The mixing weight fraction of DDAB in total surfactant is plotted horizontally and the weight fraction of *m*-xylene in the system is plotted vertically. DTAB molecules form normal-type micelles in water (W_m) whereas DDAB molecules form L_α . Upon mixing both surfactants, the phase state changes from W_m to L_α via the two-phase region.

Two kinds of L_α are formed in a water/DDAB system [20]. One of them is water-rich (less than 30 wt% of DDAB concentration at 25°C) and the other is surfactant-rich. Since the DDAB concentration at the DDAB corner is 21.3%, this L_α should be the former one. With addition of *m*-xylene, other phases are formed. A cubic liquid crystalline region lies on the upside of the W_m region in the phase diagram. Two L_α are in equilibrium above the L_α region and a three-phase region consisting of a liquid crystal, a microemulsion, and an oil phase is formed at higher *m*-xylene content. On the right-hand side of the L_α region, a narrow and skewed single-phase-microemulsion region (O_m) is formed upon addition of *m*-xylene to the oil-free L_α. W/o microemulsions are formed in a water/DDAB/oil system by adding a small amount of oil to L_α [12]. The O_m phase is also considered to be of a w/o type judging from its position in the phase diagram.

When a trace of oil is added to W_m and L_α regions, their compositions are shifted largely to the DTAB-rich side. With further addition of *m*-xylene, the W_m region moves back to the DDAB-rich side and the L_α region extends upward at a certain surfactant mixing fraction

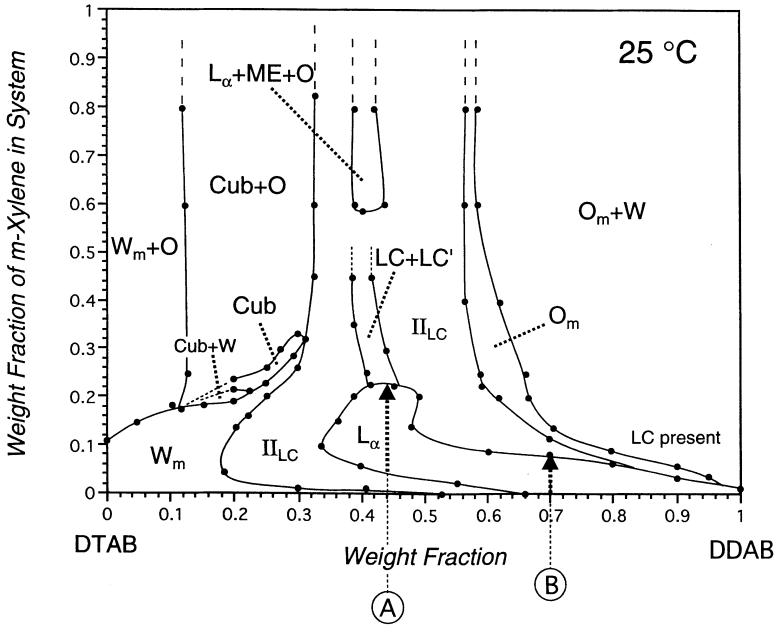

Fig. 2 Partial phase diagram of a water/DTAB/DDAB/*m*-xylene system at 25°C. The volume fraction of the lipophilic tail of a *DTAB-DDAB* mixture in aqueous surfactant solution is fixed at 0.2. W_m, W, O_m, O, Cub, L_α, II_{LC}, *LC + LC'*, and *ME* represent a normal-type micellar solution, water with monomeric surfactant, a reverse-type micellar solution, oil with monomeric surfactant, a cubic liquid crystal, a lamellar liquid crystal, a two-phase equilibrium of a birefringent liquid crystal and solvent (water or oil), a two-phase equilibrium of two kinds of birefringent liquid crystals, and a microemulsion, respectively. Small-angle X-ray scattering (SAXS) measurements were performed on lines *A* and *B*, whose DTAB/DDAB weight ratios are 56/44 and 3/7, respectively

above about 10 wt% of *m*-xylene. The O_m region also shows similar behavior. A similar phase behavior was also reported in a mixture of mono- and dioctadecyl quaternary ammonium chloride salts by Kunieda and Shinoda [21].

Since oil penetration into a surfactant palisade layer induces a negative curvature, the composition of the L_α phase first shifts to the DTAB-rich side. In other words, L_α form in more hydrophilic regions to retain zero mean curvature when penetration occurs. Hence, it seems that *m*-xylene molecules mainly penetrate into the palisade layers at an early stage of *m*-xylene addition; thereafter, all of the oil molecules swell inside the core of the bilayer. We discuss this process in detail in the following section.

Effect of oil on phase behavior

The hydrophile-lipophile property of mixed surfactants is balanced in the L_α region since a L_α has zero mean curvature. Depending on the nature of the oil, the mixing fraction of surfactant to form the L_α phase changes. The L_α regions in the partial phase diagrams for several saturated hydrocarbons having the carbon number from 8 to 14 are shown in Fig. 3.

The L_α region shifts to the DDAB-rich region with increasing oil size. The effect of the chain length of the oil corresponds to the change in temperature in polyoxyethylene-type nonionic surfactant systems [1]. The HLB temperature increases for longer-chain oils. Hence, to keep the HLB temperature constant, a more lipophilic surfactant has to be used when a long hydrocarbon is added.

Variation of the interlayer spacing of L_α as the oil content increases

The interlayer spacing of a L_α was measured at the constant DTAB/DDAB weight ratios, 56/44 and 30/70, which are shown by lines A and B in Fig. 1, respectively. The *d* values obtained are plotted in Fig. 4.

The half-thickness of the lipophilic part in a bilayer, r_{L}, and the cross-sectional area per head group at the hydrophobic interface, a_s, are calculated by Eqs. (1) and (2) [22].

$$r_L = \frac{d}{2}(\phi_L + \phi_o) \tag{1}$$

$$a_s = \frac{\nu_L}{r_L}\frac{\phi_L + \phi_o}{\phi_L}, \tag{2}$$

where ϕ_L and ϕ_o are the volume fractions of the lipophilic part of the mixed surfactant and oil in a system, respectively. ν_L is the volume of the lipophilic part of the mixed surfactant per head group. If all oil molecules penetrate into palisade layers, the r_L value should not change with addition of oil. We term this case complete penetration. In this case, the change in *d* values is simulated by the following equation derived from Eq. (1).

$$d = \frac{2r_L^0}{\phi_L + \phi_o}, \tag{3}$$

where r_L^o is the r_L value of an oil-free L_α. On the contrary, if oil molecules never penetrate, i.e., do not mix with the lipophilic tails of a surfactant in a L_α, the a_s value should not change if other conditions are fixed. We termed this case complete swelling. In this case, *d* values

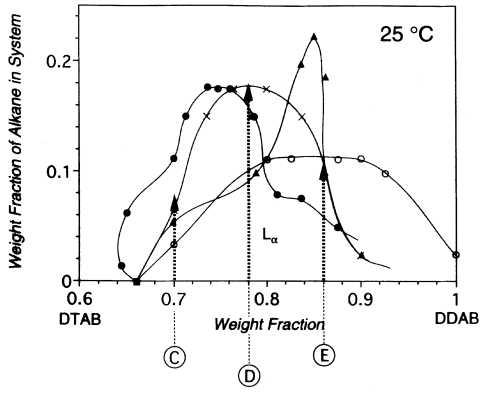

Fig. 3 The L_α region for the system with *n*-octane (*filled circles*), *n*-decane (*crosses*), *n*-dodecane (*filled triangles*), and *n*-tetradecane (*open circles*). SAXS measurements on the *n*-decane system were performed on lines *C*, *D* and *E*, whose DTAB/DDAB weight ratios are 3/7, 22/78 and 14/86, respectively

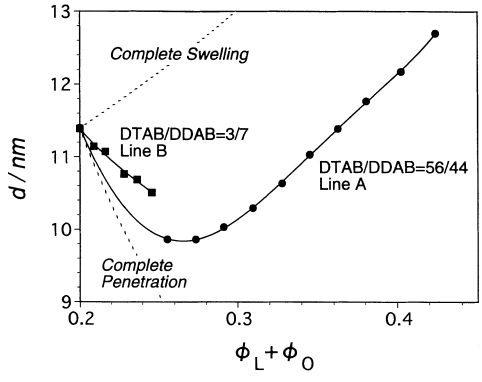

Fig. 4 Variation of interlayer spacing, *d*, with increasing *m*-xylene content on *lines A* (*filled circles*) and *B* (*filled squares*) in Fig. 2. The *upper* and *lower dotted lines* indicate the calculated *d* values for complete swelling and complete penetration, respectively

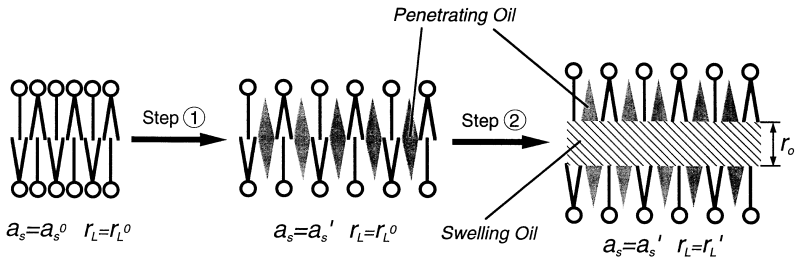

Fig. 5 Derivation scheme of the penetration parameter. Steps 1 and 2 correspond to complete penetration and complete swelling, respectively

are simulated by the following equation derived from Eqs. (1) and (2).

$$d = \frac{2\nu_L}{a_s^0 \phi_L}, \tag{4}$$

where a_s^0 is the a_s value of an oil-free L_α.

We need to know r_L^0 and a_s^0 to use Eqs. (3) and (4). However, the L_α region of the *m*-xylene system does not reach the bottom of the phase diagram at DTAB/DDAB = 56/44. We estimated r_L^0 and a_s^0 at the mixing fraction of surfactant by the following method. Interlayer spacings of oil-free L_α were measured with changing surfactant mixing fraction (measured at the bottom line in Fig. 2). As a result, d and r_L are constant in the whole L_α region, 11.4 nm and 1.14 nm, respectively. Therefore the values of d and r_L^0 at DTAB/DDAB = 56/44 can be estimated to be the same as the above values and a_s^0 is calculated to be 0.423 nm^2 by applying Eq. (2). The change in d values for complete swelling and complete penetration are calculated and plotted as dotted curves in Fig. 4.

The d values for line A drop sharply on addition of a small amount of *m*-xylene; thereafter they increase steeply through a minimum with further addition of *m*-xylene. This shows that most of the oil molecules penetrate into the palisade layer first and then the oil is solubilized in the core of the aggregates. The d values for line B decline but not as steeply as for line A; hence, the penetration behavior of *m*-xylene molecules is more drastic in the case of line A.

Evaluation of the degree of oil penetration

To evaluate the degree of oil penetration, a two-step solubilization process is considered. In the first step, oil molecules penetrate into the palisade layer and are solubilized only in the hydrocarbon tails of the surfactant, as is shown in Fig. 5.

When the volume fraction of the penetrating oil in the total added oil is defined as a penetration parameter, Pe, a_s expands to a_s' at the end of the first step, while r_L is r_L^0 (step 1 in Fig. 5). Since this process corresponds to complete penetration, a_s' is represented by the following equation derived from Eq. (2).

$$a_s' = \frac{\nu_L}{r_L^0} \frac{\phi_L + Pe\phi_o}{\phi_L} \tag{5}$$

In the second step, the rest of the oil is solubilized only in the core of the aggregates (step 2), while penetration is stopped and a_s' is kept constant. We then obtain the following equation by substituting Eq. (5) into Eq. (4).

$$Pe = \frac{2r_L^0}{\phi_o d} - \frac{\phi_L}{\phi_o} \tag{6}$$

We can estimate Pe by applying the measured d to Eq. (6).

Pe values for lines A and B are calculated by Eq. (6) and are plotted in Fig. 6.

Pe gradually declines in both cases and for line A shows greater penetration at constant $\phi_L + \phi_o$. Pe values in the *n*-decane system on the lines C, D, and E in Fig. 3 are plotted in Fig. 7.

It is shown that penetration is slightly enhanced at high DTAB ratios and penetration of *m*-xylene molecules is much greater than that of *n*-decane ones. From these results, it is clear that the degree of penetration mainly depends on the surfactant mixing ratio and the nature of the oil.

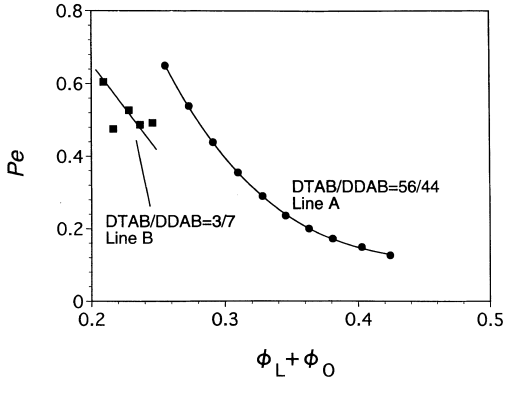

Fig. 6 Variation of the penetration parameter, Pe, with increasing *m*-xylene content on *lines A* (*filled circles*) and *B* (*filled* squares)

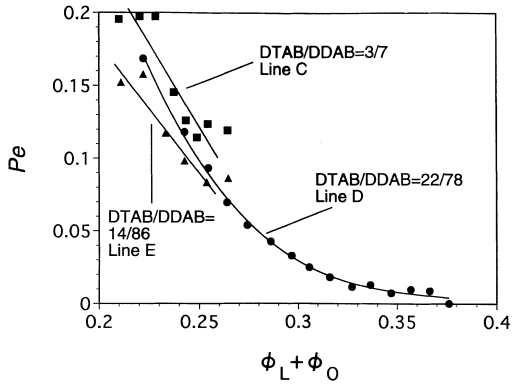

Fig. 7 Variation of the penetration parameter, *Pe*, with increasing *n*-decane content on *lines C* (*filled squares*), *D* (*filled circles*), and *E* (*filled triangles*)

Precise examination of oil penetration behavior

To understand the oil penetration behavior in detail, the oil thickness in the core (shown in Fig. 5), r_o, is estimated by the following equation:

$$r_o = 2r_L - 2r_L^0 \tag{7}$$

The results are shown in Fig. 8.

It is expected that r_o would increase constantly after solubilization in a palisade layer is saturated. In fact, a straight line is obtained after a certain amount of *m*-xylene is added as is shown in Fig. 8. This corresponds to the crooked range of the L_α region in Fig. 2. This result strongly suggests that first the palisade layer is saturated with oil and then the surfactant layers are monotonically separated with further increase in oil content.

We obtain the amount of oil solubilized in the palisade layer per unit of two head groups, 0.30 nm^3, by extrapolating the straight line to $r_o = 0$. This value is about one-fourth of the volume of the lipophilic tail per unit of two head groups, 1.16 nm^3. The same analysis was carried out for the *n*-decane system and the results are shown in Table 1. The decane penetration is much smaller than for *m*-xylene molecules as explained before.

The volume for line D is the largest value among the three mixing fractions of surfactants in the *n*-decane system. This is related to the fact that the solubilization capacity in L_α reaches a maximum at line D as is shown in Fig. 3.

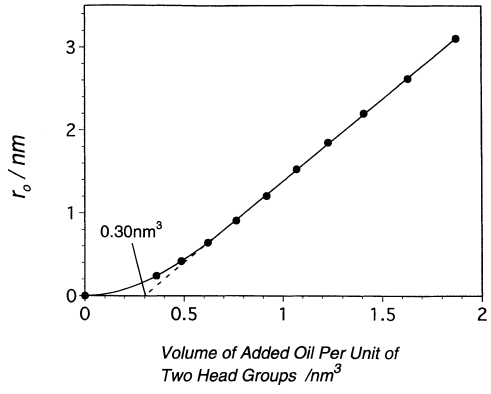

Fig. 8 Variation of the oil thickness in the core, r_o, with increasing *m*-xylene content on line A

Summary

In an aqueous solution of a DTAB-DDAB mixture, normal-type micelles are formed on the DTAB-rich side whereas L_α are formed on the DDAB-rich side. Upon addition of *m*-xylene to the aqueous solution, other phases such as cubic liquid crystals and microemulsions are formed. The L_α region shifts toward higher DTAB ratios in mixed surfactants with the addition of oil, and an oil having a smaller molecular size induces a more drastic shift of the L_α region in the phase diagram.

From SAXS measurement, the effective cross-sectional area per surfactant head group, a_s, and the thickness of the lipophilic part of a bilayer in a L_α, r_L, are evaluated. It is considered that a_s is expanded and r_L is constant in the case of complete penetration and vice versa in the case of complete swelling. The degree of oil penetration is evaluated by penetration parameters. The degree of penetration is enhanced with increasing DTAB ratio and decreasing molecular size of the oil. The thickness of a layer of *swelling oil* in a L_α, r_o, is evaluated. From the variation of r_o with the amount of oil added, it was found that most of the *m*-xylene molecules penetrate into the surfactant layer at an early stage of addition; thereafter, *m*-xylene is solubilized in the core of the bilayer. The volume of penetrating oil is largest when the total oil solubilization capacity in L_α reaches a maximum. Furthermore, the *m*-xylene volume solubilized in the surfactant palisade layer is much greater than that in the *n*-decane system.

Table 1 Maximum volume of penetrating oil per unit of two surfactant head groups

Oil used	*m*-Xylene	*n*-Decane		
DDAB fraction in mixed surfactant	0.44	0.7	0.78	0.86
Volume of penetrating oil/nm^3	0.30	0.04	0.07	0.02

References

1. Kunieda H, Shinoda K (1985) J Colloid Interface Sci 107:107
2. Kunieda H, Sato Y (1992) In: Friberg SE, Lindman B (ed) Organized solutions. Dekker, New York, pp 70–73
3. Evans DF, Wennerström H (1994) The colloidal domain. VCH, New York, p 460
4. Hoffmann H, Ulbricht W (1989) J Colloid Interface Sci 129:388
5. Strey R, Glatter O, Schubert KV, Kaler EW (1996) J Chem Phys 105:1175
6. Eastoe J, Dong J, Hetherington KJ, Steytler D, Heenan R (1996) J Chem Soc Faraday Trans 92:65
7. Eastoe J, Hetherington KJ, Sharpe D, Dong J, Heenan R, Steytler D (1996) Langmuir 12:3876
8. Kunieda H, Nakano A, Pes MA (1995) Langmuir 11:3302
9. Kunieda H, Aoki R (1996) Langmuir 12:5796
10. Kunieda H, Yamagata M (1993) Langmuir 9:3345
11. Kunieda H, Nakano A, Akimaru M (1995) J Colloid Interface Sci 170:78
12. Fontell K, Ceglie A, Lindman B, Ninham B (1986) Acta Chem Scand A 40:247
13. Chen SJ, Evans DF, Ninham BW, Mitchell DJ, Blum FD, Pickup S (1986) J Phys Chem 90:842
14. Zemb TN, Hyde ST, Derian P, Barnes IS, Ninham BW (1987) J Phys Chem 91:3814
15. Barnes IS, Hyde ST, Ninham BW, Derian P, Drifford M, Zemb TN (1988) J Phys Chem 92:2286
16. Monduzzi M, Caboi F, Larche F, Olsson U (1997) Langmuir 13:2184
17. Kunieda H, Shigeta K, Ozawa K, Suzuki M (1997) J Phys Chem 101:7952
19. Fontell K (1974) In: Gray GW, Winsor PA (ed) Liquid crystals and plastic crystals. Wiley, London, p 88
20. Warr GG, Sen R, Evans DF (1988) J Phys Chem 92:774
21. Kunieda H, Shinoda K (1978) J Phys Chem 82:1710
22. Kunieda H, Ozawa K, Huang KL (1998) J Phys Chem B 102:831